

# A CD36-dependent pathway enhances macrophage and adipose tissue inflammation and impairs insulin signalling

David J. Kennedy<sup>1</sup>, Sai Kuchibhotla<sup>1</sup>, Kristen M. Westfall<sup>1</sup>, Roy L. Silverstein<sup>1</sup>, Richard E. Morton<sup>1</sup>, and Maria Febbraio<sup>2\*</sup>

<sup>1</sup>Department of Cell Biology, Lerner Research Institute, Cleveland Clinic, Cleveland, OH 44195, USA; and <sup>2</sup>Department of Molecular Cardiology, Lerner Research Institute, Cleveland Clinic, Cleveland, OH 44195, USA

Received 30 July 2010; revised 8 November 2010; accepted 10 November 2010; online publish-ahead-of-print 18 November 2010

Time for primary review: 37 days

<b>Aims</b>	Obesity and hyperlipidaemia are associated with insulin resistance (IR); however, the mechanisms responsible remain incompletely understood. Pro-atherogenic hyperlipidaemic states are characterized by inflammation, oxidant stress, and pathophysiologic oxidized lipids, including ligands for the scavenger receptor CD36. Here we tested the hypothesis that the absence of CD36 protects mice from IR associated with diet-induced obesity and hyperlipidaemia.
<b>Methods and results</b>	Adipose tissue from <i>CD36</i> <sup>-/-</sup> mice demonstrated a less inflammatory phenotype and improved insulin signalling <i>in vivo</i> and at the level of the adipocyte and macrophage. The pathophysiologic ligand oxidized low-density lipoprotein (oxLDL) activated c-Jun N-terminal kinase (JNK) and disrupted insulin signalling in both adipocytes and macrophages in a CD36-dependent manner. Macrophages isolated from <i>CD36</i> <sup>-/-</sup> mice after high-fat diet feeding elicited less JNK activation and inhibition of insulin signalling in adipocytes after co-culture compared with wild-type macrophages.
<b>Conclusion</b>	These data suggest that a CD36-dependent inflammatory paracrine loop between adipocytes and macrophages facilitates chronic inflammation and contributes to IR common in obesity and dyslipidaemia.
<b>Keywords</b>	CD36 • Obesity • Insulin resistance • Macrophages • Adipocytes

## 1. Introduction

Because of its role in fatty acid transport and expression on insulin-sensitive tissues, contribution of the class B scavenger receptor CD36 to insulin resistance (IR) has been the focus of study. A limited number of human studies have shown associations of CD36 with impaired insulin sensitivity.<sup>1–3</sup> In rodent models, CD36 interaction with fatty acids may play a role in the pathogenesis of metabolic disorders such as IR, obesity, and non-alcoholic hepatic steatosis, and absence of CD36-mediated lipid uptake in muscle or liver is capable of preventing diet-induced lipotoxicity.<sup>4–6</sup> CD36 recognizes a variety of ligands generated in settings of IR which may similarly contribute to pathogenesis. For example, pro-atherogenic hyperlipidaemic states are characterized by the generation of pathophysiologically oxidized

lipids which are highly associated with IR.<sup>7,8</sup> We showed that phospholipids truncated in the sn-2 position present in oxidatively modified low-density lipoprotein (oxLDL) provide the recognition site for CD36 and subsequent signalling events, and uptake results in macrophage foam cell formation *in vitro* and *in vivo*,<sup>9,10</sup> and provide a mechanistic link between oxidant stress, platelet hypersensitivity, and thrombosis.<sup>11</sup> In this way, we hypothesize that oxidized lipids may link hyperlipidaemia, obesity, and IR.

Because inflammation and oxidant stress associated with obesity are particularly manifest at the level of adipose tissue<sup>12</sup> where CD36 is highly expressed, we tested whether pathological ligands for CD36 disrupt insulin signalling in adipocytes through activation of CD36-dependent signalling pathways. We hypothesized that pro-atherogenic hyperlipidaemic states would potentiate a

\* Corresponding author. Tel: +1 216 444 5605; fax: +1 216 445 8204. Email: febbram@ccf.org

Published on behalf of the European Society of Cardiology. All rights reserved. © The Author 2010. For permissions please email: journals.permissions@oup.com.

The online version of this article has been published under an open access model. Users are entitled to use, reproduce, disseminate, or display the open access version of this article for non-commercial purposes provided that the original authorship is properly and fully attributed; the Journal, Learned Society and Oxford University Press are attributed as the original place of publication with correct citation details given; if an article is subsequently reproduced or disseminated not in its entirety but only in part or as a derivative work this must be clearly indicated. For commercial re-use, please contact journals.permissions@oup.com.

CD36-dependent inflammatory paracrine loop between adipocytes and their associated macrophages, facilitating the development of chronic inflammation in adipose tissue that underlies the insulin-resistant state common to obesity and cardiovascular disease. We describe here that absence of CD36 protects mice from IR associated with diet-induced obesity and hyperlipidaemia, and that in adipocytes and macrophages, oxLDL activates c-Jun N-terminal kinase (JNK) and disrupts insulin signalling in a CD36-dependent manner.

## 2. Methods

### 2.1 Animals and diets

Littermate-derived wild-type (WT) and *CD36*<sup>-/-</sup> (10× backcrossed to C57Bl/6), *apoE*<sup>-/-</sup> and *apoE*<sup>-/-</sup>/*CD36*<sup>-/-</sup> (7× backcrossed to C57Bl/6), and *LDLR*<sup>-/-</sup> and *LDLR*<sup>-/-</sup>/*CD36*<sup>-/-</sup> mice (8× backcrossed to C57Bl/6) were as previously described<sup>10,13</sup> except further backcrossed as indicated. *Lyn*<sup>-/-</sup> (6× backcrossed to C57Bl/6) and *Fyn*<sup>-/-</sup> (1× backcrossed to C57Bl/6) mice were from the Jackson Laboratory. *MyD88*<sup>-/-</sup> mice (7× backcrossed to C57Bl/6) were a generous gift from Clifford Harding (Case Western Reserve University). Age- and sex-matched mice were fed a high-fat diet (HFD) (36%, w/w, adjusted calories from fat, Bio-Serv S3282) for 8–12 weeks or in the case of *LDLR*<sup>-/-</sup> strains, a high-fat/high-cholesterol diet (Harlan Teklad 96121); controls were maintained on chow (Harlan Teklad, TD 2918). All animal procedures were priorly approved by the Institutional Animal Care and Use Committee, carried out in an AAALAC accredited facility, and the investigation conforms with the Guide for the Care and Use of Laboratory Animals published by the US National Institutes of Health (NIH Publication No. 85-23, revised 1996).

### 2.2 *In vitro* metabolic analyses

Tail vein blood for plasma was collected 1 week prior to sacrifice after overnight fast in 5 mM EDTA-dipotassium salt. Non-esterified fatty acids and triacylglycerol were assayed using kits from Wako, and fasting insulin was measured with the Ultrasensitive Mouse Insulin ELISA (ALPCO). Plasma lipoprotein profiles were determined by fast protein liquid chromatography of 10  $\mu$ L aliquots on two Superose 6 columns with continuous online detection of cholesterol in the eluant.<sup>14</sup>

For glucose tolerance testing (GTT), mice were fasted overnight and injected (intraperitoneal) with 2 mg glucose/g of body weight. Tail vein blood glucose was measured using a One Touch Basic glucometer (Johnson & Johnson). For insulin tolerance tests, mice were challenged with an intraperitoneal injection of human insulin (0.75 mU/g, Novulin-R) after a 4 h fast. For biochemical analysis of insulin signalling, human insulin (5 mU/g) was injected intravenously after a 4 h fast. After 5 min, gonadal WAT, quadriceps, and liver were isolated and snap-frozen in liquid nitrogen.

### 2.3 Reagents and cell culture

Tissue culture media, supplements, and reagents were as described in detail in Supplementary material online, Methods. 3T3L1 and stromal vascular fraction (SVF) pre-adipocytes were differentiated and cultured using the Adipogenesis Kit (Cayman Chemical). Isolation and culture of resident peritoneal macrophages (RPM) and SVF pre-adipocytes are described in Supplementary material online, Methods. For all *in vitro* experiments examining insulin signalling,

cells were treated with 100 nM insulin for the final 20 min prior to harvest.

### 2.4 Detection of reactive oxygen species, cytokine/chemokines, and related assays

Oxidative burst in pooled RPM and SVF macrophages was measured using Fc OxyBURST Green assay (Molecular Probes; described in detail in Supplementary material online, Methods). Plasma cytokine levels were determined by a multiplex ELISA cytokine array (Q-Plex Mouse Cytokine Array-Screen IR 16-plex; Quansys Biosciences) and plasma interferon (IFN- $\gamma$ ) was confirmed by ELISA (Bender Medsystems). Cytokine levels in conditioned media (CM) pooled from RPM and 3T3L1 adipocytes were determined using the Proteome Profiler Mouse Cytokine Array, Panel A (R&D Systems). Arginase activity was assayed using the QuantiChrom™ Arginase Assay (BioAssay Systems); free glycerol was assayed using the Free Glycerol Reagent (Sigma).

### 2.5 Glucose uptake

Glucose uptake into 3T3L1 adipocytes was measured using 2-NBDG (Molecular Probes), a fluorescent derivative of glucose as previously described<sup>15,16</sup> and described in detail in Supplementary material online, Methods.

### 2.6 *In vitro* migration assay

Migration of RPM was measured in a modified Boyden chamber migration assay using Transwell inserts with an 8  $\mu$ M porous membrane (Corning). Cells were loaded into the migration chamber with CM from WT or *CD36*<sup>-/-</sup> adipocytes treated for 12 h  $\pm$  oxLDL. After allowing cell migration for 16 h, cells were removed from the upper side of the membranes, and nuclei of migratory cells on the lower side of the membrane were stained with 4',6-diamidino-2-phenylindole. The nuclei were visualized by fluorescence microscopy, and the average number of migratory cells was determined from averaging four fields.

### 2.7 Preparation of tissue homogenates, cell lysate, and immunoblotting

Equal amounts of protein were prepared using standard biochemical methods (described in detail in Supplementary material online, Methods) and subjected to sodium dodecyl sulfate–polyacrylamide gel electrophoresis and electrotransfer to Immobilon-P membranes (Millipore). Membranes were incubated with the following antibodies: phospho-SAPK/JNK (Thr<sup>183</sup>Tyr<sup>185</sup>), phospho-c-Jun (Ser<sup>63</sup>), SAPK/JNK, phospho-IRS-1 (Ser<sup>307</sup>), IRS-1, phospho-AKT (Ser<sup>473</sup>), AKT, and I $\kappa$ B $\alpha$  (Cell Signaling Technology); Fyn, Lyn, and actin (Santa Cruz Biotechnology); phospho-IRS-1 (Tyr<sup>608</sup>) (Millipore); iNOS (BD Bioscience); CD36 (Novus Biologicals). Detection was performed with the SNAP i.d.™ Protein Detection System (Millipore) and Super Signal Chemiluminescent Substrate Products (Pierce), and band intensity was analyzed by densitometry (ImageJ v1.37).

### 2.8 Histology and immunohistochemistry

Immunohistochemistry was performed on deparaffinized 5  $\mu$ m serial sections incubated in 3% hydrogen peroxide followed by 5% milk, and then overnight (4°C) with anti-MAC-2 (1:500; Cedarlane) or isotype control. Histochemical reactions were performed using the EnVision® Doublestain System (DakoCytomation) and counterstained with haematoxylin.

## 2.9 Statistical analysis

Data presented are mean  $\pm$  standard error of the mean. Data obtained were first tested for normality using the D'Agostino–Pearson omnibus test. If the data did not pass the normality test, the Tukey test (for multiple groups) or the Mann–Whitney rank sum test was used to compare the data. If the data did pass the normality test, parametric comparisons were performed. If more than two groups were compared, one-way analysis of variance was performed prior to comparison of individual groups with the unpaired Student's *t*-test with Bonferroni's correction for multiple comparisons. If only two groups of normal data were compared, the Student's *t*-test was used without correction. Statistical analysis was performed using GraphPad Prism<sup>®</sup>.

## 3. Results

### 3.1 CD36 contributes to impaired glucose tolerance and obesity

We measured parameters of glucose and lipid metabolism in age-matched male and female mice fed the HFD for 8 weeks. Before diet treatment, all cleared a bolus of glucose within 2 h (not shown). After, GTT was greatly impaired in WT vs. *CD36*<sup>-/-</sup> mice (Figure 1A); area under the curve (AUC) was significantly greater in WT males (37%) and females (33%). Fasting hyperinsulinaemia was significantly less ( $P < 0.01$ ) in *CD36*<sup>-/-</sup> animals (Supplementary material online, Figure S1), as was fasting plasma free glycerol, a measure of lipolysis (14% lower,  $P < 0.05$ ) (Supplementary material

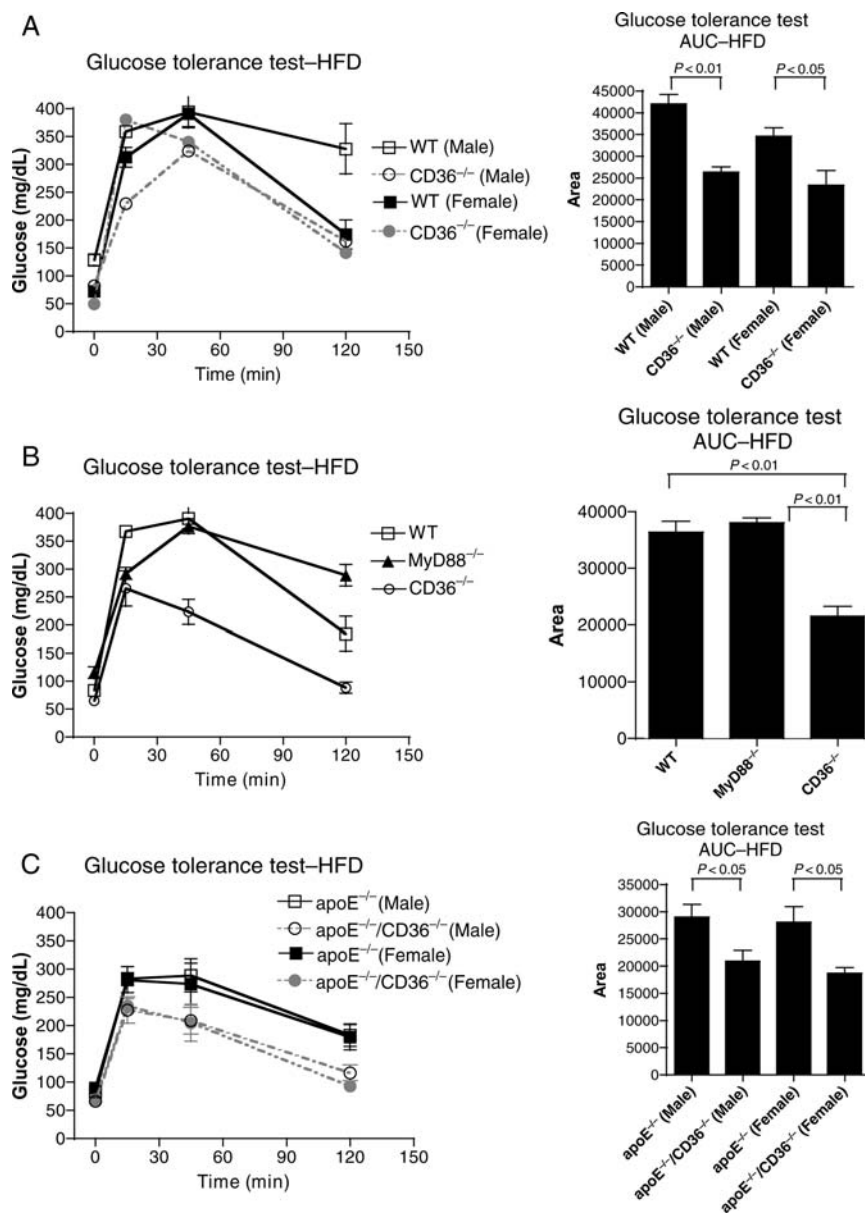


**Figure 1** Protection from diet-induced IR in *CD36*<sup>-/-</sup> mice. Intraperitoneal GTT for mice of the indicated sex and genotype fed the HFD for 8 weeks (A, C) or male mice at 4 weeks (B). GTT AUC analysis is shown on right.  $n \geq 5$  per group.

online, Figure S2). Interestingly, WT and  $CD36^{-/-}$  mice had equivalent levels of free fatty acids and LDL, suggesting that metabolic improvements in  $CD36^{-/-}$  mice were not due to grossly detectable changes in circulating ligands (Supplementary material online, Table S1). Despite consuming similar amounts of food (Supplementary material online, Figure S3),  $CD36^{-/-}$  mice were protected from HFD-induced weight gain (Supplementary material online, Figure S4) and adiposity (36% lower,  $P < 0.05$ ) (Supplementary material online, Figure S5).

CD36 has been shown to be a co-receptor for Toll-like receptors (TLRs).<sup>17–19</sup> TLR signalling by a subset of ligands, including oxLDL and fatty acids, is propagated by recruitment of the universal adaptor molecule MyD88.<sup>20</sup>  $MyD88^{-/-}$  mice fed the HFD were not protected from an insulin-resistant phenotype (Figure 1B; Supplementary material online, Figure S6).

To control for degree of adiposity as a potential confounder, we studied 12-week HFD-fed apolipoprotein E null ( $apoE^{-/-}$ ) and  $apoE^{-/-}/CD36^{-/-}$  mice; these animals have equivalent body weights and adiposity (Supplementary material online, Figure S7). GTT showed greater impairment (29% greater AUC,  $P < 0.05$ ) in male and female  $apoE^{-/-}$  mice (Figure 1C). There was a two-fold increase in the level of fasting insulin in  $apoE^{-/-}$  mice; levels in  $apoE^{-/-}/CD36^{-/-}$  animals were similar to NC-fed controls (Supplementary material online, Figure S8). Using a second hyperlipidaemic model, the LDL receptor null ( $LDLR^{-/-}$ ), we observed pronounced impairment of glucose tolerance in  $LDLR^{-/-}$  vs.  $LDLR^{-/-}/CD36^{-/-}$

mice fed a high-fat, high-cholesterol (1.25%) diet (Supplementary material online, Figure S9).

### 3.2 CD36 contributes to impaired insulin signalling in adipose tissue

To identify sites of IR, HFD-fed WT and  $CD36^{-/-}$  mice were injected with insulin, and tissues harvested for biochemical analysis. There was decreased phosphorylation of insulin-stimulated Akt, indicating impaired insulin signalling, in gonadal white adipose tissue (WAT; Figure 2A), but not in the quadriceps (Supplementary material online, Figure S10) or liver (Supplementary material online, Figure S11) of WT vs.  $CD36^{-/-}$  mice.

Metabolic stress from HFD feeding is also known to cause activation of the regulatory mitogen-activated protein (MAP) kinase JNK and trigger the development of IR.<sup>21</sup> WAT from HFD-fed  $CD36^{-/-}$  mice had significantly less JNK activation vs. WT ( $P < 0.05$ ) (Figure 2B) and a similar decrease was observed in HFD-fed  $apoE^{-/-}/CD36^{-/-}$  vs.  $apoE^{-/-}$  mice (Supplementary material online, Figure S12).

JNK can directly induce IR by serine phosphorylation of the adapter protein, insulin receptor substrate 1 (IRS-1), at inhibitory sites which in turn decreases IRS-1 tyrosine phosphorylation and blocks insulin receptor signalling.<sup>22</sup> Adipose tissue from WT mice had three-fold less ( $P < 0.05$ ) IRS-1 tyrosine phosphorylation ( $pY^{608}$ ) vs.  $CD36^{-/-}$  mice (Figure 2C). Similar impairments in insulin signalling were

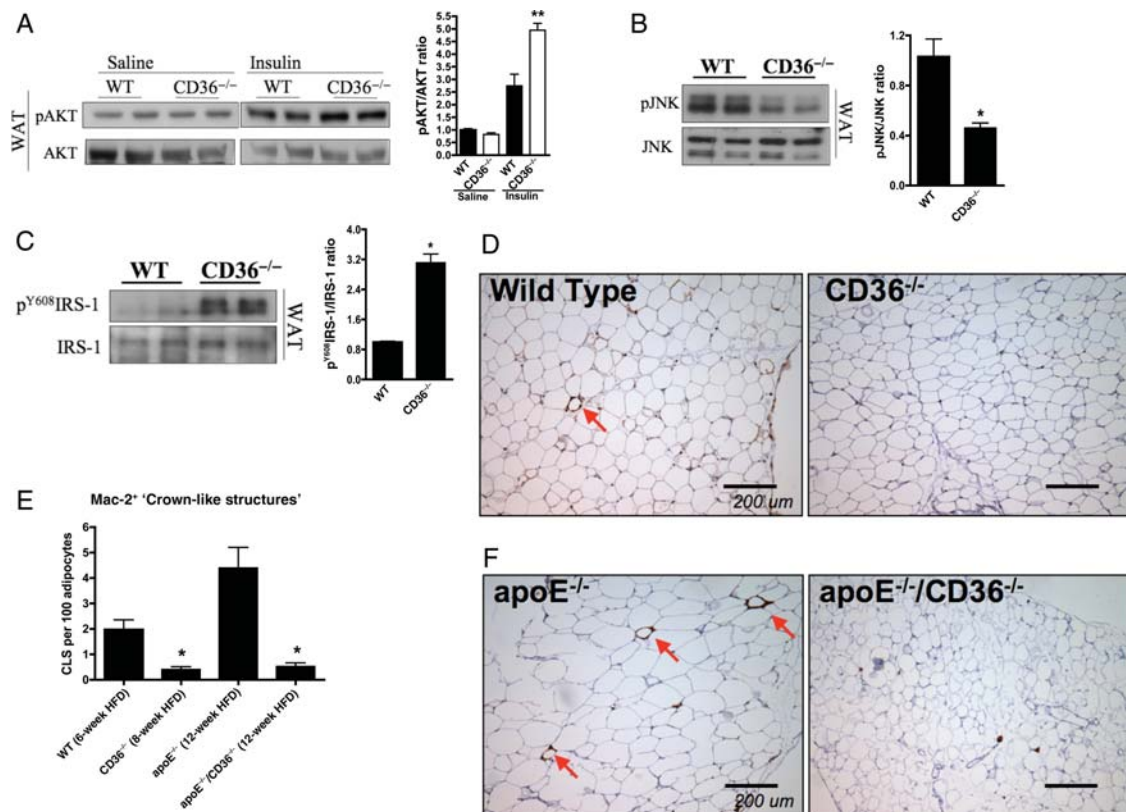


**Figure 2** CD36 contributes to inflammation and macrophage infiltration in adipose tissue after HFD. *In vivo* insulin signalling assay of AKT phosphorylation in (A) WAT of 8-week HFD  $CD36^{-/-}$  vs. WT mice. Representative immunoblots (left) and quantification (right) of (B) JNK phosphorylation and (C) IRS-1 tyrosine phosphorylation from WAT of 8-week HFD mice. (D, F) MAC-2 staining of representative WAT sections from HFD mice, and (E) quantification of CLS (arrows) expressed as a percentage of CLS/100 adipocytes averaged from four separate fields. \* $P < 0.05$ ; \*\* $P < 0.01$  vs. WT;  $n \geq 5$  per group.

observed *in vivo* in adipose tissue, liver, and muscle in HFD-fed *apoE*<sup>-/-</sup>/*CD36*<sup>-/-</sup> vs. *apoE*<sup>-/-</sup> mice (not shown).

### 3.3 CD36 contributes to inflammation and macrophage infiltration in adipose tissue

Plasma from HFD-fed *CD36*<sup>-/-</sup> mice had lower levels of inflammatory cytokines and chemokines vs. WT mice, including IFN- $\gamma$  ( $27.2 \pm 1.0$  vs.  $35.6 \pm 3.4$  pg/mL,  $P < 0.05$ ), a Th1 cytokine involved in fat inflammation. Infiltrating macrophages contribute to IR during HFD-induced obesity<sup>23</sup> and monocyte chemotactic protein (MCP)-1, a key chemokine involved in the recruitment of macrophages, was elevated in WT vs. *CD36*<sup>-/-</sup> plasma ( $4.4 \pm 1.1$  vs.  $2.2 \pm 0.2$  pg/mL,  $P < 0.05$ ). Histological examination of gonadal WAT revealed four-fold fewer ( $P < 0.01$ ) Mac-2 expressing 'crown-like structures' (CLS; Figure 2D and E), hallmarks of adipose tissue inflammation. WAT from HFD-fed *apoE*<sup>-/-</sup>/*CD36*<sup>-/-</sup> mice had eight-fold fewer ( $P < 0.01$ ) CLS vs. *apoE*<sup>-/-</sup> WAT (Figure 2E and F).

### 3.4 CD36 contributes to an M1 phenotype

An important feature of adipose tissue inflammation and IR is the predominance of a classical M1 pro-inflammatory macrophage vs. an M2 anti-inflammatory tissue-residing macrophage.<sup>23</sup> M1 macrophages are characterized by enhanced pro-inflammatory cytokine production as well as a shift in the iNOS/arginase balance to iNOS, which favours the generation of reactive oxygen species (ROS) such as NO. RPM from HFD-fed WT mice showed two-fold or more increases in several key inflammatory cytokines, including IFN- $\gamma$ , MCP-1, MIP-1 $\alpha$ , and TNF- $\alpha$ , vs. *CD36*<sup>-/-</sup> macrophages, under basal conditions (Supplementary material online, Table S2) and in response to oxLDL (Supplementary material online, Table S3). OxLDL-stimulated WT RPM demonstrated significantly greater ROS production (Figure 3A), and macrophages isolated from the adipose SVF of HFD-fed WT mice also had greater ROS production, both basally and in response to oxLDL (Supplementary material online, Figure S13). RPM from HFD-fed *CD36*<sup>-/-</sup> mice had nearly two-fold more ( $P < 0.01$ ) arginase activity vs. WT (Supplementary material online, Figure S14). Additionally, *CD36*<sup>-/-</sup> macrophages expressed significantly less iNOS and NF $\kappa$ B (assessed indirectly as less I $\kappa$ B $\alpha$  degradation) (Figure 3B). OxLDL treatment was associated with a 50% increase in the expression of iNOS in WT macrophages, an effect that was absent in *CD36*<sup>-/-</sup> macrophages (Supplementary material online, Figure S15). In addition, WAT from HFD-fed *CD36*<sup>-/-</sup> mice

demonstrated 90% decreased iNOS expression ( $P < 0.01$ ) and four-fold greater arginase activity ( $P < 0.05$ ) vs. WT WAT (Supplementary material online, Figures S16 and 17).

Similar to our primary cell data, oxLDL treatment of the classic adipocyte cell line, 3T3L1, resulted in at least two-fold increase in several cytokines/chemokines important for macrophage recruitment, including G-CSF, sICAM, IL-6, and MIP-2 (Supplementary material online, Figure S18).

### 3.5 OxLDL promotes a CD36-dependent IR phenotype in adipocytes

OxLDL increased JNK phosphorylation in 3T3L1 adipocytes and this effect was inhibited by pre-incubation with a monoclonal antibody (mAb) to CD36 (Supplementary material online, Figure S19). We observed a 50% increase ( $P < 0.05$ ) in p-cJun, a downstream target of JNK, and this was attenuated by pre-treatment with either mAb to CD36 or a pharmacologic inhibitor of JNK kinase (Figure 4A). OxLDL treatment induced a two-fold increase ( $P < 0.05$ ) in the inhibitory serine phosphorylation (S<sup>307</sup>) of IRS-1 and this effect was also attenuated by mAb to CD36 and JNK kinase inhibition (Figure 4B). Similarly, in primary adipocytes isolated from WT gonadal WAT, oxLDL induced JNK activation, and this was completely abrogated in *CD36*<sup>-/-</sup> cells (Figure 4C). We next differentiated adipocytes from the SVF of gonadal WAT and observed that oxLDL treatment induced a two-fold increase in p-cJun in WT but not *CD36*<sup>-/-</sup> adipocytes (Supplementary material online, Figure S20).

In addition to oxLDL, we also examined the effects of other CD36 ligands on insulin signalling in adipocytes, including advanced glycation end products in bovine serum albumin (AGE-BSA), free fatty acids (FA), and fatty acids exposed to the myeloperoxidase (MPO)/H<sub>2</sub>O<sub>2</sub>/NO<sub>2</sub>-generating system (oxFA). Using adipocytes differentiated from the SVF, we observed that both FA and oxFA treatment induced ~50% decrease in insulin-stimulated p-AKT levels in WT and *MyD88*<sup>-/-</sup> adipocytes ( $P < 0.05$ ) but had no effect on *CD36*<sup>-/-</sup> adipocytes (Supplementary material online, Figure S21). It is likely, however, that FA were already significantly oxidized, because precautions are not taken by the manufacturer to prevent this. AGE-BSA did not induce significant changes in JNK activation or AKT phosphorylation (not shown).

CD36-dependent activation of MAP kinases has been previously shown to be mediated by upstream activation of Src family kinases in other cell types, and we explored whether this was the case in

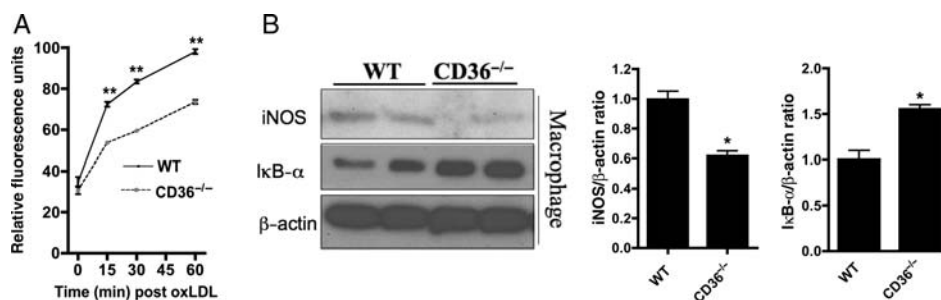


**Figure 3** CD36 contributes to a pro-inflammatory phenotype in macrophages after HFD. (A) Oxidative burst in RPM isolated from 8-week HFD female mice treated with 50  $\mu$ g/mL oxLDL over 60 min as described in Supplementary material online, Methods. (B) Representative immunoblots (left) and quantification (right) of iNOS and I $\kappa$ B $\alpha$  expression in RPM. \* $P < 0.05$ ; \*\* $P < 0.01$  vs. WT;  $n \geq 5$  per group.

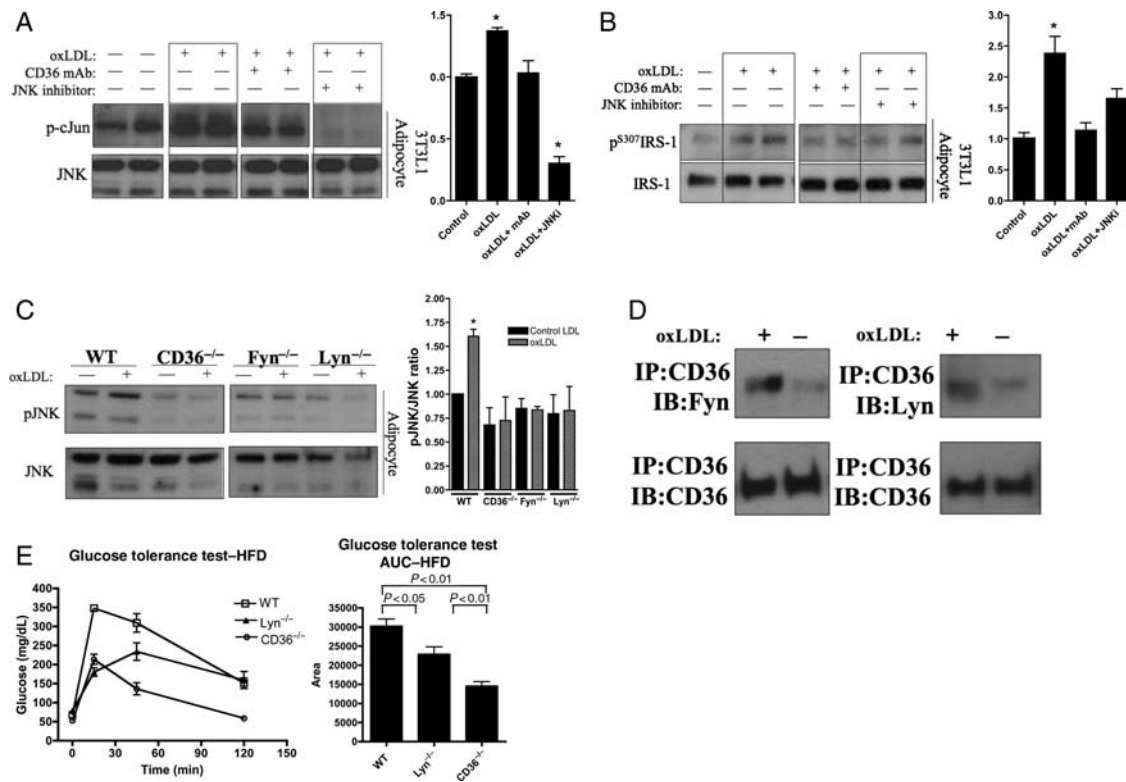


**Figure 4** OxLDL promotes CD36-dependent molecular and physiologic impairment of insulin signalling in adipocytes. Representative immunoblots (left) and quantification (right) of oxLDL-induced increases in phospho-c-Jun (A) and inhibitory phosphorylation of IRS-1 at serine 307 (B) in a CD36-dependent manner in 3T3L1 adipocytes treated for 60 min with 50  $\mu$ g/mL oxLDL and pre-incubated with a mAb to CD36 (5  $\mu$ g/mL) or a pharmacologic inhibitor of JNK kinase activity (SP600125, 20  $\mu$ M). \*  $P < 0.05$  vs. control, quantification summarized from at least three independent experiments. (C) JNK phosphorylation in primary adipocytes isolated from mice and treated for 15 min with 50  $\mu$ g/mL oxLDL. (D) 3T3L1 adipocytes treated with 50  $\mu$ g/mL oxLDL or control for 15 min were immunoprecipitated with a mAb to CD36 and then immunoblotted with polyclonal Abs to Fyn, Lyn, or CD36. (E) GTT and AUC analysis (right) of 4-week HFD female mice of the indicated genotype;  $n \geq 5$  per group.

adipocytes. Pharmacologic inhibition of tyrosine kinases with Herbi-mycin A and Src kinases with PP2 were both capable of attenuating JNK phosphorylation in 3T3L1 adipocytes (Supplementary material online, Figure S22). Furthermore, oxLDL-induced inhibitory serine phosphorylation of IRS-1 was also diminished by treatment with PP2 (Supplementary material online, Figure S23).

We tested the involvement of Src family kinases previously shown to have a role in oxLDL-CD36 responses (Fyn, Lyn) using adipocytes isolated from knockout mice. Similar to  $CD36^{-/-}$ , the oxLDL-induced increase in p-JNK was abrogated in adipocytes from  $Fyn^{-/-}$  and  $Lyn^{-/-}$  mice (Figure 4C). Co-immunoprecipitation revealed that oxLDL treatment of 3T3L1 adipocytes increased the association of CD36 with Fyn and Lyn (Figure 4D). These data suggest that either Fyn or Lyn is sufficient for JNK activation. In order to confirm involvement *in vivo*, GTT was performed on 4-week HFD-fed  $Lyn^{-/-}$  mice.  $Lyn^{-/-}$  mice exhibited improved glucose tolerance vs. WT (Figure 4E), but not to the degree observed in  $CD36^{-/-}$  mice. Given the redundancy in Src kinases, however, it is not surprising that individual deletion of Lyn does not produce a phenotype which completely mimics CD36 deletion.

### 3.6 oxLDL impairs adipocyte insulin responses in a CD36-dependent manner

To understand the functional implications of oxLDL-mediated changes in p-JNK, p-IRS-1, and p-AKT, we examined the effect of

oxLDL on physiologic correlates of insulin sensitivity in 3T3L1 adipocytes. OxLDL treatment decreased glucose uptake by  $\sim 15\%$  ( $P < 0.05$ ), decreased adiponectin secretion by  $\sim 45\%$  ( $P < 0.01$ ), and increased adipocyte lipolysis ( $P < 0.05$ ) (Supplementary material online, Figures S24–S26). Each of these effects was attenuated by pre-incubation with CD36 mAb.

### 3.7 HFD impairs macrophage insulin signalling in a CD36-dependent manner *in vivo*

We isolated RPM after HFD feeding to assess the effect of CD36 ligands *in vivo*. We observed increased phosphorylation of cJun and decreased phosphorylation of AKT (Figure 5A and B) in RPM from WT vs.  $CD36^{-/-}$  mice.

### 3.8 CD36 contributes to impaired insulin signalling in co-cultured adipocytes and macrophages

Obesity is associated with infiltration of fat by macrophages, suggesting they contribute to the inflammatory phenotype.<sup>12,23</sup> We co-cultured 3T3L1 adipocytes with RPM isolated from HFD-fed  $apoE^{-/-}$  or  $apoE^{-/-}/CD36^{-/-}$  mice. Adipocytes co-cultured with direct contact to  $apoE^{-/-}$  macrophages showed increased p-cJun and decreased

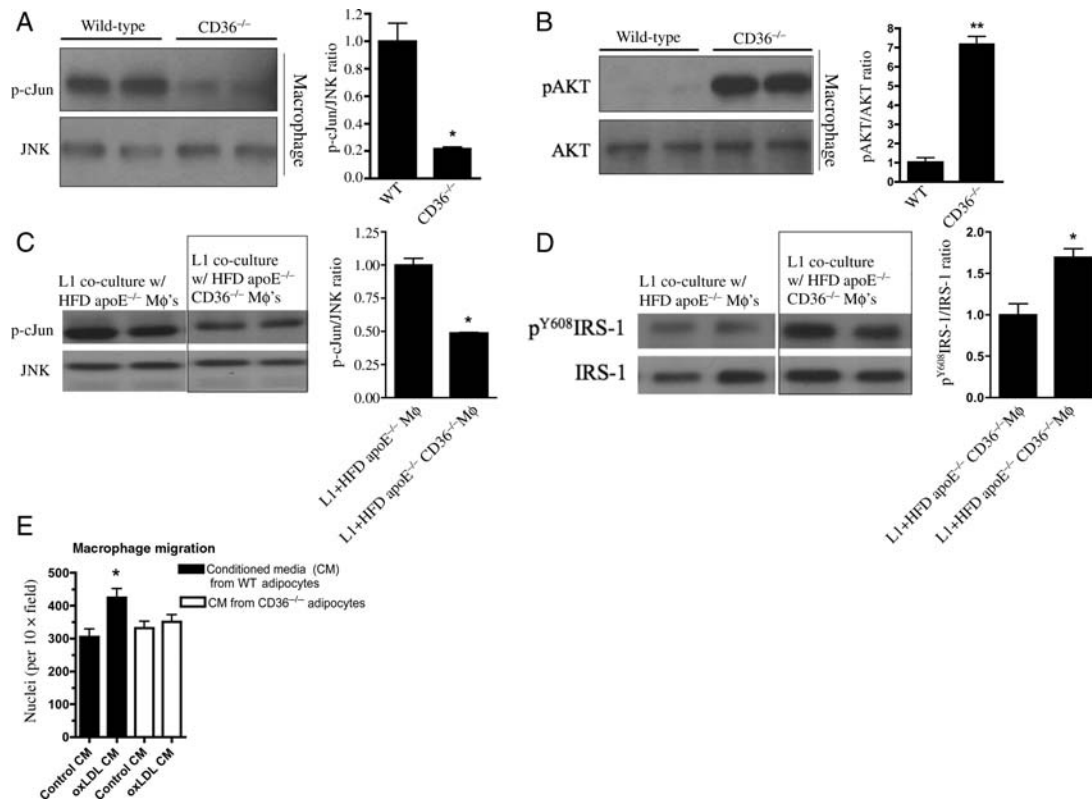


**Figure 5** CD36 contributes to inflammation and impaired insulin signalling in macrophages with and without adipocyte co-culture. Representative immunoblots (left) and quantification (right) demonstrating CD36-dependent increased (A) phospho-c-Jun and decreased (B) phospho-AKT in RPM cultured from 4-week HFD mice for 12 h. \* $P < 0.05$ ; \*\* $P < 0.01$  vs. WT;  $n \geq 5$  per group. Representative immunoblots (left) and quantification (right) for (C) phospho-c-Jun and (D) phospho-tyrosine-IRS-1 from 3T3L1 adipocytes co-cultured for 24 h with  $0.5 \times 10^6$  RPM isolated from 8-week HFD mice of the indicated genotypes. (E) Macrophage migration to CM from WT and  $CD36^{-/-}$  adipocytes which had been previously exposed to oxLDL or control media as described in Supplementary material online, Methods. \* $P < 0.05$  vs. control.

tyrosine phosphorylation of IRS-1 ( $pY^{608}$ IRS-1) vs. those co-cultured with  $apoE^{-/-}/CD36^{-/-}$  macrophages (Figures 5C and D).

We next used an *in vitro* migration assay to assess the functional interaction between macrophages and adipocytes exposed to CD36 ligands. WT and  $CD36^{-/-}$  adipocytes were exposed to oxLDL or control, washed extensively, and then incubated in serum-free media. This CM was collected and placed in the bottom of a transwell migration chamber. WT macrophages showed significantly increased migration when exposed to CM from WT adipocytes treated with oxLDL compared with macrophages exposed to CM from  $CD36^{-/-}$  adipocytes treated with either oxLDL or control media ( $P < 0.05$ , Figure 5E).

## 4. Discussion

In this report, we provide multiple lines of *in vitro* and *in vivo* evidence supporting a mechanistic link between inflammation, oxidative stress, hyperlipidaemia, and IR mediated by the type 2 scavenger receptor CD36. This work supports the hypothesis that CD36 not only recognizes pathological ligands and removes them, a physiologic role, but in circumstances of obesity and hyperlipidaemia, these ligands also signal via CD36 to affect inflammatory and insulin signalling pathways in a pathophysiological response. This newly recognized role of CD36 has the potential to be targeted by therapeutics and thus provides a

relevant strategy to the clinically significant problem of cardiovascular morbidity and mortality associated with diabetes and IR. Our findings suggest a novel role for CD36 in mediating a pro-inflammatory signalling loop between macrophages and adipocytes that contributes to IR in hyperlipidaemic settings.

$CD36^{-/-}$  mice in several backgrounds were protected from chronic inflammation induced by HFD feeding: they demonstrated significantly lower levels of key circulating inflammatory cytokines, as well as a decrease in CLS in adipose tissue. After HFD feeding, macrophages from  $CD36^{-/-}$  mice secreted less pro-inflammatory cytokines and ROS, had increased arginase activity, and decreased expression of key inflammatory mediators. Indeed,  $CD36^{-/-}$  macrophages themselves reflected attenuation of defects in the insulin signalling pathway after HFD feeding. Direct co-culture of WT macrophages from HFD-fed mice with 3T3L1 adipocytes gave rise to increased activation of JNK and impaired insulin signalling in adipocytes and this was significantly abrogated in adipocytes incubated with macrophages lacking CD36. Further, CM from WT but not  $CD36^{-/-}$  adipocytes stimulated with oxLDL had important functional consequences for macrophage migration: migration of macrophages was enhanced by exposure to WT but not  $CD36^{-/-}$  adipocyte CM, suggesting that soluble factors released from adipocytes in response to CD36 signalling may play an important role in macrophage recruitment and inflammation in adipose tissue as observed in *in vivo* studies.

Although our work and work by others have shown that macrophage scavenger receptors are sometimes associated with an anti-inflammatory phenotype because of their role in the clearance of apoptotic cells and resolution of inflammation,<sup>17,24,25</sup> the data herein indicate that CD36 is not necessarily a classic antiphlogistic receptor. To be sure, our data do not exclude a role for CD36 in M2 macrophages, where it has been shown to be upregulated by PPAR $\gamma$  and others have suggested may be involved in the increase in fatty acid oxidation associated with the M2 phenotype.<sup>26</sup> Indeed, TLR4 has also been shown to be highly expressed in M2 macrophages, yet it plays a critical role in inflammation as well.<sup>27</sup>

The contribution of CD36 to IR is controversial. Some genetic cohort studies suggest that CD36 protects against IR,<sup>28</sup> whereas other do not.<sup>29</sup> A quantitative trait locus in the region encoding the CD36 gene has been linked to pathological components of the metabolic syndrome.<sup>1</sup> Love-Gregory *et al.*<sup>2</sup> have demonstrated the association of several single-nucleotide polymorphisms across this region—including those that are documented to result in CD36 deficiency—which conferred protection against the metabolic syndrome. Thus, whether these CD36 polymorphisms represent a gain or loss of function or how they interact with other genetic determinants needs to be established. The discrepancy between CD36 *protecting from* or *pre-disposing to* IR may be accounted for by whether or not a pro-inflammatory environment generates pathologic CD36 ligands, and the tissues involved.

Diabetes and IR increase inflammation and ROS which may contribute to atherosclerosis by both creating modified LDL ligands and causing endothelial dysfunction. The increase in pro-inflammatory cytokines noted in our study and others<sup>30</sup> may not only increase macrophage migration into adipose tissue, but also into the adventitia of the vasculature. We have demonstrated that these proinflammatory mediators may also cause significant CD36-dependent cytoskeletal rearrangements which contribute to macrophage trapping.<sup>31</sup> The clinical sequelae of this dysfunction has important implications for hypertension, myocardial infarction, and stroke. Thus, diabetes and IR may contribute to a spectrum of cardiovascular diseases, and therapeutics focused on CD36 signalling cascades provide an attractive target because of its established involvement in several of these processes.

The data in this report support a pro-inflammatory role for CD36 in the setting of pro-atherogenic, hyperlipidaemic conditions and agree with previous evidence from our lab and others.<sup>13,30,32</sup> This finding is not surprising given the fact that CD36 recognizes ligands that trigger an inflammatory innate immune response and that others have shown that CD36 is a co-receptor for certain TLR ligands including specific lipid and lipoprotein components of Gram-positive bacteria cell walls, staphylococcal and mycobacterial organisms,  $\beta$ -glucans on fungal pathogens, and erythrocytes infected with falciparum malaria.<sup>17,33,34</sup> Ligand engagement of CD36 in these settings can activate classic TLR signalling cascades resulting in NF $\kappa$ B activation and secretion of pro-inflammatory cytokines.<sup>18,19</sup>

Some studies have suggested that adipose tissue macrophages are both necessary and sufficient for the development of IR in obesity. Macrophage-specific deletion of JNK<sup>35</sup> or deletion of MCP-1 or its receptor, CCR2<sup>36,37</sup> reverses HFD-induced IR. However, inflammatory signals from the macrophage compartment alone may not be mediators of diet-induced IR, as other reports have concluded that only JNK inactivation in the parenchyma or adipose tissue is capable of restoring insulin sensitivity after HFD feeding.<sup>38,39</sup> In any

case, work by others established that JNK plays an essential role in the development of IR in obesity<sup>21</sup> where its activation leads to phosphorylation of IRS-1 on serine 307. Increased p<sup>S307</sup>IRS-1 uncouples IRS-1 from the insulin receptor and decreases IRS-1 tyrosine phosphorylation at sites necessary for interaction with PI-3K, thereby impairing insulin action. We observed that in addition to improvements in physiologic correlates of IR such as glucose tolerance and lipolysis, HFD-fed CD36<sup>-/-</sup> mice also had decreased JNK activation and improved insulin signalling in adipose tissue. Additionally, we demonstrated *in vitro* that oxLDL was able to activate JNK and increase inhibitory serine phosphorylation of IRS-1 in adipocytes in a CD36-dependent manner. Further, we showed that oxLDL-induced CD36-dependent changes in adipocytes associated with important physiologic correlates of IR *in vitro* including impaired glucose uptake, adiponectin secretion, and increased lipolysis. The hypothesis that oxLDL participates in the development of IR is supported by the work of Scazzocchio *et al.*<sup>8</sup> in that they demonstrated that oxLDL impaired both glucose uptake and the recruitment of GLUT4 to plasma membranes in adipocytes and that these effects were attenuated by pre-treatment with a mAb to CD36. Although our studies have focused on oxLDL, the results do not exclude effects of other CD36 ligands, because the HFD model generates multiple insults. Although AGE-BSA did not appear to appreciably disrupt insulin signalling, saturated fatty acids such as palmitate did demonstrate CD36-dependent interference with insulin-stimulated pAKT (Supplementary material online, Figure S21).

Work by our group and others has shown that modified lipoproteins, such as oxLDL, arise as byproducts during an inflammatory response and play a key role in cardiovascular disease.<sup>40,41</sup> Podrez *et al.*<sup>9</sup> characterized the structural basis of CD36 recognition sites on oxLDL as modified phosphatidylcholine species, and more recently, Greenberg *et al.*<sup>42</sup> have proposed the 'lipid-whisker model' to explain CD36 recognition of these truncated sn-2 fatty acids present in phospholipids of various head group classifications. These recognition sites are also found on apoptotic cells and effete rod outer segments in the eye, and both must be cleared to prevent disease, thus representing a homeostatic function of CD36.<sup>25,43</sup> The pattern recognition function of CD36 has been conserved throughout evolution across a diverse range of species.<sup>44</sup> This suggests a 'molecular mimicry' paradigm underlying our central hypothesis: although evolution has selected for the ability of CD36 to be an effective lipopeptide sensor, inflammation associated with diet-induced obesity now generates ligands equally capable of stimulating this receptor. The results of the current study expand a purely 'lipotoxic' view of HFD-induced IR suggested by others and now identifies CD36 as a central signalling molecule upstream of JNK activation in the cellular pathway to IR induced by a HFD and CD36 ligands such as oxLDL.

In the current study, we used a variety of *in vitro* and *in vivo* approaches, including pharmacologic inhibition, immunoprecipitation, and genetic deletion of Src kinases to demonstrate that most probably Fyn and Lyn associate with CD36 in adipocytes and act upstream of JNK signalling. This is consistent with our previous observations of CD36 signalling elsewhere.<sup>45,46</sup>

Adipocytes express typical macrophage proteins including almost their entire repertoire of cytokines and chemokines and in the current study we noted significant increases in several adipocyte cytokines/chemokines elicited by oxLDL stimulation of importance for macrophage recruitment. To further examine the contribution of macrophage CD36 to HFD-induced IR, we analyzed data from a



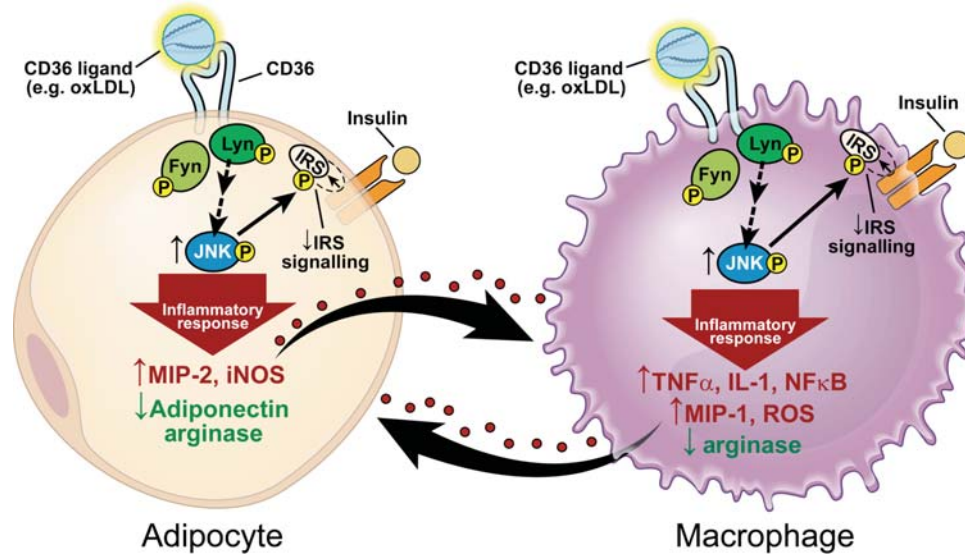


**Figure 6** CD36 contributes to inflammation and impaired insulin signalling in adipocytes and macrophages.

prior study from our group in which bone marrow (BM) transplantation was used to determine the role of macrophage CD36 in atherosclerosis.<sup>10</sup> Male *apoE*<sup>-/-</sup> mice receiving *apoE*<sup>-/-</sup>/*CD36*<sup>-/-</sup> BM had a trend towards improved GTT after 12 weeks of HFD feeding ( $P = 0.054$ ) when compared with those receiving *apoE*<sup>-/-</sup> BM. This data coupled with the results of the current study suggest that in addition to other compartments such as adipose tissue, macrophage CD36 may play an important role in IR associated with HFD feeding.

Our data provide evidence that absence of CD36 protects mice from IR associated with diet-induced obesity and hyperlipidaemia and that CD36 ligands such as oxLDL are capable of mediating a CD36-dependent inflammatory paracrine loop between adipocytes and their associated macrophages. This facilitates chronic inflammation in adipose tissue and contributes to the IR common in obesity and dyslipidaemia (Figure 6).

## Supplementary material

Supplementary material is available at *Cardiovascular Research* online.

## Acknowledgment

Some data were presented in abstract form at the 2008 and 2009 Experimental Biology Meetings.

**Conflict of interest:** none.

## Funding

This work was supported by the NIH (P01 HL087018, P01 HL46403, HL072942 to M.F. and R.L.S.); the AHA Great Rivers Affiliate (0825685D to D.J.K.); the Lerner Research Institute's David and Lindsay Morgenthaler Endowed Fellowship (to D.J.K.). Funding to pay the Open Access publication charge was provided by the Cleveland Clinic.

## References

1. An P, Freedman BI, Hanis CL, Chen YD, Weder AB, Schork NJ *et al.* Genome-wide linkage scans for fasting glucose, insulin, and insulin resistance in the NHLBI Family

Blood Pressure Program: evidence of linkages to chromosome 7q36 and 19q13 from meta-analysis. *Diabetes* 2005;**54**:909–914.

2. Love-Gregory L, Sherva R, Sun L, Wasson J, Schappe T, Doria A *et al.* Variants in CD36 gene associate with metabolic syndrome and high-density lipoprotein cholesterol. *Hum Mol Genet* 2008;**17**:1695–1704.
3. Bonen A, Tandon NN, Glatz JF, Luiken JJ, Heigenhauser GJ. The fatty acid transporter FAT/CD36 is upregulated in subcutaneous and visceral adipose tissues in human obesity and type 2 diabetes. *Int J Obes (Lond)* 2006;**30**:877–883.
4. Goudriaan JR, Dahlmans VE, Teusink B, Ouwens DM, Febbraio M, Maassen JA *et al.* CD36 deficiency increases insulin sensitivity in muscle, but induces insulin resistance in liver in mice. *J Lipid Res* 2003;**44**:2270–2277.
5. Hajri T, Han XX, Bonen A, Abumrad NA. Defective fatty acid uptake modulates insulin responsiveness and metabolic responses to diet in CD36-null mice. *J Clin Invest* 2002;**109**:1381–1389.
6. Koonen DP, Jacobs RL, Febbraio M, Young ME, Soltys CL, Ong H *et al.* Increased hepatic CD36 expression contributes to dyslipidemia associated with diet-induced obesity. *Diabetes* 2007;**56**:2863–2871.
7. Holvoet P, Lee DH, Steffes M, Gross M, Jacobs DR Jr. Association between circulating oxidized LDL and incidence of the metabolic syndrome. *J Am Med Assoc* 2008;**299**:2287–2293.
8. Scazzocchio B, Vari R, D'Archivio M, Santangelo C, Filesi C, Giovannini C *et al.* Oxidized LDL impair adipocyte response to insulin by activating serine/threonine kinases. *J Lipid Res* 2009;**50**:832–845.
9. Podrez EA, Poliakov E, Shen Z, Zhang R, Deng Y, Sun M *et al.* A novel family of atherogenic oxidized phospholipids promotes macrophage foam cell formation via the scavenger receptor CD36 and is enriched in atherosclerotic lesions. *J Biol Chem* 2002;**277**:38517–38523.
10. Febbraio M, Guy E, Silverstein RL. Stem cell transplantation reveals absence of macrophage CD36 is protective against atherosclerosis. *Arterioscler Thromb Vasc Biol* 2004;**24**:2333–2338.
11. Podrez EA, Byzova TV, Febbraio M, Salomon RG, Ma Y, Valiyaveetil M *et al.* Platelet CD36 links hyperlipidemia, oxidant stress and prothrombotic phenotype. *Nat Med* 2007;**13**:1086–1095.
12. Wellen KE, Hotamisligil GS. Obesity-induced inflammatory changes in adipose tissue. *J Clin Invest* 2003;**112**:1785–1788.
13. Kennedy DJ, Kuchibhotla SD, Guy E, Park YM, Nimako G, Vanegas D *et al.* Dietary cholesterol plays role in CD36-mediated atherogenesis in LDLR-knockout mice. *Arterioscler Thromb Vasc Biol* 2009;**29**:1481–1487.
14. Garber DW, Kulkarni KR, Anantharamaiah GM. A sensitive and convenient method for lipoprotein profile analysis of mouse plasma samples. *J Lipid Res* 2000;**41**:1020–1026.
15. Leira F, Louzao MC, Vieites JM, Botana LM, Vieytes MR. Fluorescent microplate cell assay to measure uptake and metabolism of glucose in normal human lung fibroblasts. *Toxicol In Vitro* 2002;**16**:267–273.
16. Zou C, Wang Y, Shen Z. 2-NBDG as a fluorescent indicator for direct glucose uptake measurement. *J Biochem Biophys Methods* 2005;**64**:207–215.

17. Hoebe K, Georgel P, Rutschmann S, Du X, Mudd S, Crozat K *et al*. CD36 is a sensor of diacylglycerides. *Nature* 2005;**433**:523–527.
18. Stewart CR, Stuart LM, Wilkinson K, van Gils JM, Deng J, Halle A *et al*. CD36 ligands promote sterile inflammation through assembly of Toll-like receptor 4 and 6 heterodimer. *Nat Immunol* 2010;**11**:155–161.
19. Triantafilou M, Gamper FG, Haston RM, Mouratis MA, Morath S, Hartung T *et al*. Membrane sorting of toll-like receptor (TLR)-2/6 and TLR2/1 heterodimers at cell surface determines heterotypic associations with CD36 and intracellular targeting. *J Biol Chem* 2006;**281**:31002–31011.
20. Bjorkbacka H, Kunjathoor VV, Moore KJ, Koehn S, Ordija CM, Lee MA *et al*. Reduced atherosclerosis in MyD88-null mice links elevated serum cholesterol levels to activation of innate immunity signaling pathways. *Nat Med* 2004;**10**:416–421.
21. Hirosumi J, Tuncman G, Chang L, Gorgun CZ, Uysal KT, Maeda K *et al*. A central role for JNK in obesity and insulin resistance. *Nature* 2002;**420**:333–336.
22. Aguirre V, Uchida T, Yenush L, Davis R, White MF. The c-Jun NH(2)-terminal kinase promotes insulin resistance during association with insulin receptor substrate-1 and phosphorylation of Ser(307). *J Biol Chem* 2000;**275**:9047–9054.
23. Lumeng CN, Bodzin JL, Saltiel AR. Obesity induces phenotypic switch in adipose tissue macrophage polarization. *J Clin Invest* 2007;**117**:175–184.
24. Means TK, Mylonakis E, Tampakakis E, Colvin RA, Seung E, Puckett L *et al*. Evolutionarily conserved recognition and innate immunity to fungal pathogens by scavenger receptors SCARF1 and CD36. *J Exp Med* 2009;**206**:637–653.
25. Savill J, Hogg N, Ren Y, Haslett C. Thrombospondin cooperates with CD36 and the vitronectin receptor in macrophage recognition of neutrophils undergoing apoptosis. *J Clin Invest* 1992;**90**:1513–1522.
26. Odegaard JI, Ricardo-Gonzalez RR, Goforth MH, Morel CR, Subramanian V, Mukundan L *et al*. Macrophage-specific PPAR $\gamma$  controls alternative activation and improves insulin resistance. *Nature* 2007;**447**:1116–1120.
27. Bassaganya-Riera J, Misyak S, Guri AJ, Hontecillas R. PPAR $\gamma$  highly expressed in F4/80(hi) adipose tissue macrophages and dampens adipose-tissue inflammation. *Cell Immunol* 2009;**258**:138–146.
28. Furuhashi M, Ura N, Nakata T, Tanaka T, Shimamoto K. Genotype in human CD36 deficiency and diabetes mellitus. *Diabet Med* 2004;**21**:952–953.
29. Yanai H, Chiba H, Morimoto M, Jamieson GA, Matsuno K. Type I CD36 deficiency in humans not associated with insulin resistance syndrome. *Thromb Haemost* 2000;**83**:786.
30. Manning-Tobin JJ, Moore KJ, Seimon TA, Bell SA, Sharuk M, Alvarez-Leite JJ *et al*. Loss of SR-A and CD36 activity reduces atherosclerotic lesion complexity without abrogating foam cell formation in hyperlipidemic mice. *Arterioscler Thromb Vasc Biol* 2009;**29**:19–26.
31. Park YM, Febbraio M, Silverstein RL. CD36 modulates migration of mouse and human macrophages in response to oxidized LDL and may contribute to macrophage trapping in arterial intima. *J Clin Invest* 2009;**119**:136–145.
32. Martin-Fuentes P, Civeira F, Recalde D, Garcia-Otin AL, Jarauta E, Marzo I *et al*. Individual variation of scavenger receptor expression in human macrophages with oxidized LDL associated with differential inflammatory response. *J Immunol* 2007;**179**:3242–3248.
33. Philips JA, Rubin EJ, Perrimon N. *Drosophila* RNAi screen reveals CD36 family member required for mycobacterial infection. *Science* 2005;**309**:1251–1253.
34. Stuart LM, Deng J, Silver JM, Takahashi K, Tseng AA, Hennessy EJ *et al*. Response to *Staphylococcus aureus* requires CD36-mediated phagocytosis triggered by COOH-terminal cytoplasmic domain. *J Cell Biol* 2005;**170**:477–485.
35. Solinas G, Vilcu C, Neels JG, Bandyopadhyay GK, Luo JL, Naugler W *et al*. JNK1 in hematopoietically derived cells contributes to diet-induced inflammation and insulin resistance without affecting obesity. *Cell Metab* 2007;**6**:386–397.
36. Kanda H, Tateya S, Tamori Y, Kotani K, Hiasa K, Kitazawa R *et al*. MCP-1 contributes to macrophage infiltration into adipose tissue, insulin resistance, and hepatic steatosis in obesity. *J Clin Invest* 2006;**116**:1494–1505.
37. Weisberg SP, Hunter D, Huber R, Lemieux J, Slaymaker S, Vaddi K *et al*. CCR2 modulates inflammatory and metabolic effects of high-fat feeding. *J Clin Invest* 2006;**116**:115–124.
38. Sabio G, Das M, Mora A, Zhang Z, Jun JY, Ko HJ *et al*. A stress signaling pathway in adipose tissue regulates hepatic insulin resistance. *Science* 2008;**322**:1539–1543.
39. Vallerie SN, Furuhashi M, Fucho R, Hotamisligil GS. A predominant role for parenchymal c-Jun amino terminal kinase in the regulation of systemic insulin sensitivity. *PLoS One* 2008;**3**:e3151.
40. Silverstein RL, Febbraio M. CD36 and atherosclerosis. *Curr Opin Lipidol* 2000;**11**:483–491.
41. Witztum JL, Steinberg D. Role of oxidized LDL in atherogenesis. *J Clin Invest* 1991;**88**:1785–1792.
42. Greenberg ME, Li XM, Gugiu BG, Gu X, Qin J, Salomon RG *et al*. The lipid whisker model of the structure of oxidized cell membranes. *J Biol Chem* 2008;**283**:2385–2396.
43. Ryeom SW, Sparrow JR, Silverstein RL. CD36 participates in phagocytosis of rod outer segments by retinal pigment epithelium. *J Cell Sci* 1996;**109**:387–395.
44. Gordon S. Pattern recognition receptors: doubling up for the innate immune response. *Cell* 2002;**111**:927–930.
45. Chen K, Febbraio M, Li W, Silverstein RL. A specific CD36-dependent signaling pathway required for platelet activation by oxidized LDL. *Circ Res* 2008;**102**:1512–1519.
46. Rahaman SO, Lennon DJ, Febbraio M, Podrez EA, Hazen SL, Silverstein RL. A CD36-dependent signaling cascade is necessary for macrophage foam cell formation. *Cell Metab* 2006;**4**:211–221.